8.7 MODELING MICROSTRUCTURAL EVOLUTION IN NEUTRON IRRADIATED TUNGSTEN — X. Hu, Y. Katoh (Oak Ridge National Laboratory), D. Xu, L.L. Snead, B.D. Wirth (University of Tennessee, Knoxville)

OBJECTIVE

The objective of this project is to develop a self-consistent cluster dynamics model based on diffusion-reaction rate theory to simulate the microstructural evolution of tungsten subject to neutron irradiation, thereby, to aid in understanding the degradation mechanism of tungsten and developing practical plasma facing materials.

SUMMARY

A diffusion-reaction cluster dynamics model based on rate theory was applied to depict the distribution of vacancy and interstitial clusters in tungsten following low temperature (90°C) and low dose (0.03 dpa) neutron irradiation. For experimental data to validate the developed model, *ex situ* characterization of vacancy defects using positron lifetime spectroscopy (PLS) was performed following one-hour anneals at 400, 500, 650, 800, 1000, 1150, and 1300°C for the high purity (110) single crystalline tungsten. TEM observations on tungsten after selected anneal conditions were also performed to determine the dislocation loop population. The data from microstructural observation were then used to validate the developed model as well as the kinetics and energetics parameters describing defect interactions in tungsten obtained from atomistic simulations.

PROGRESS AND STATUS

Introduction

Tungsten plasma facing components (PFCs) in fusion reactors will experience an extreme environment including high temperature and thermal flux, intense radiation, and significant cyclic thermal stress loading. Significant defect accumulations and the resulting degradation of thermo-mechanical properties are expected for tungsten during and after exposure to intense radiation. The combined effects of radiation damage and heat load in tungsten must be understood through a coordinated experimental and modeling approach due to a lack of fusion-relevant testing capability [1]. The effect of irradiation on materials' microstructure and properties is an inherently multiscale phenomenon [2], requiring the close integration of various modeling methods. In a recent review paper [3], Wirth et al. summarized their recent modeling efforts to closely integrate the modeling results with high-resolution experimental characterization of the evolving radiation-damaged microstructure. In order to compare with experimental data directly, it is common to model the neutron irradiation process by using a mean field diffusion-reaction cluster dynamics model, which involves the use of energetics and kinetics parameters obtained from atomistic simulations, such as DFT, MD, and yields the defect cluster population [3] [4] .

Model Description

Free vacancies and self-interstitial atoms (SIAs), as well as spherical vacancy clusters and SIA clusters in the form of planar, prismatic dislocation loops, are continuously generated and evolve in pure tungsten under neutron irradiation [5] [6], therefore, only intrinsic defects and their clusters are considered in this model. Given that the energy transfer cross section of energetic neutrons is very small (~10^{-24} cm^2), the defect generation and evolution are assumed to be homogeneous and no spatial dependence will be considered here. Therefore, the concentration of each cluster is only a function of time, and ordinary differential equations are employed to depict the defect evolution. The generic form to describe the evolution of a cluster is

$$\frac{dC_i}{dt} = f' \; P_i + G_T + G_E - A_T - A_E \qquad (1)$$

where C_i refers to the volumetric concentration (in 1/m^3) of the i-th cluster, f is neutron flux (in neutron/m^2/sec), P_i is the production 'probability' of the i-th cluster by neutron irradiation, *G* refers to the collective generation rates, *A* indicates the collective annihilation rates, *T* refers to generation or annihilation by trapping events, and *E* refers to generation or annihilation by emission events. The detailed construction of the coupled system of ODEs can be found in References [3] [4] .The mathematical expressions for the binary interactions can also be found in these two references.

The external source of intrinsic point defects and the corresponding clusters is the neutron irradiation induced collision cascade occurring inside the tungsten. A recent systematic MD study of cascade in tungsten [7] clearly showed that energetic PKAs directly produce small interstitial and vacancy clusters rather than isolated Frenkel pairs. Therefore, intra-cascade cluster production was used to determine the defect production probability, same as the work presented in [4]. PKA spectrum in tungsten neutron-irradiated in HFIR was calculated by using SPECTER, the results of which are shown in Figure 1.

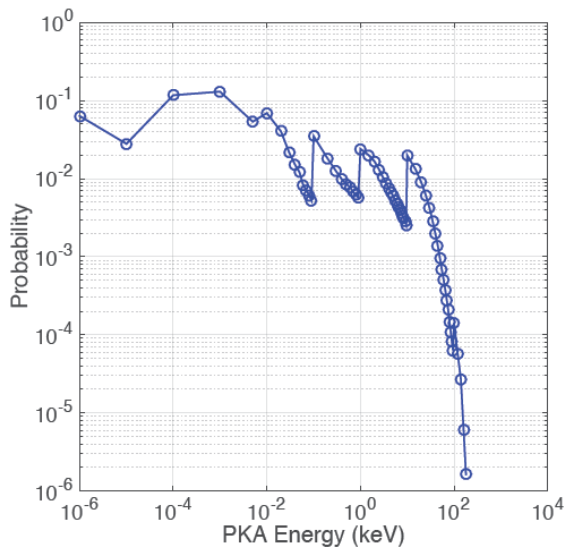

Figure 1. PKA spectrum in neutron irradiated tungsten in HFIR.

The surviving Frenkel pairs from the displacement cascade induced by the PKAs with different energies were calculated based on the empirical expressions summarized in [7], in the form of

$$N_F = \begin{cases} 0.49\times\left(\frac{E_{PKA}}{E_d}\right)^{0.74} & \text{if } E_{PKA}<35 \text{ keV} \\ 0.02\times\left(\frac{E_{PKA}}{E_d}\right)^{1.30} & \text{if } E_{PKA}\geq 35 \text{ keV} \end{cases} \quad (2)$$

Consequently, the survived point defects in the cascade were partitioned into small clusters according to the clustering fractions obtained from [7]. The numbers of clusters produced by all PKA energies were then multiplied by the corresponding probabilities shown in Figure 1. The resulting cluster production 'probability' in unit of 1/PKA is listed in Table 1.

Table 1. Intra-cascade defect cluster production rate

Vacancy cluster size	Production Probability (1/PKA)	Production rate (1/cm^3/s)	Interstitial cluster size	Production Probability (1/PKA)	Production rate (1/cm^3/s)
1	1.03E+00	5.116E+15	1	1.31E+00	1.48E+15
2	1.73E-01	8.620E+14	2	1.74E-01	1.96E+14
3	8.36E-02	4.164E+14	3	4.66E-02	5.26E+13
4	3.82E-02	1.904E+14	4	3.02E-02	3.40E+13
5	2.39E-02	1.188E+14	5	1.53E-02	1.73E+13
6	1.58E-02	7.876E+13	6	6.50E-03	7.34E+12
7	1.01E-02	5.033E+13	7	5.93E-03	6.69E+12
8	4.38E-03	2.182E+13	8	2.58E-03	2.92E+12
9	1.82E-03	9.040E+12	9	1.86E-03	2.10E+12
10	2.30E-03	1.147E+13	10	1.36E-03	1.54E+12
11	8.02E-04	3.995E+12	11	1.08E-03	1.22E+12
12	2.02E-03	1.007E+13	12	1.56E-03	1.76E+12
13	1.22E-04	6.075E+11	13	6.87E-04	7.75E+11
14	1.07E-03	5.334E+12	14	3.90E-04	4.41E+11
16	4.47E-04	2.226E+12	15	4.18E-04	4.72E+11
17	4.43E-05	2.206E+11	16	1.14E-03	1.28E+12
18	1.08E-04	5.357E+11	17	2.66E-05	3.00E+10
19	3.90E-04	1.940E+12	18	1.65E-04	1.86E+11
20	2.40E-04	1.197E+12	20	7.11E-05	8.02E+10
21	5.77E-05	2.872E+11	21	2.03E-04	2.29E+11
22	1.08E-04	5.365E+11	22	9.55E-05	1.08E+11
24	1.33E-05	6.630E+10	23	3.37E-04	3.81E+11
27	4.44E-05	2.209E+11	24	2.60E-04	2.93E+11
29	1.90E-04	9.453E+11	25	8.21E-05	9.26E+10
30	1.08E-04	5.370E+11	26	4.44E-05	5.01E+10
34	1.52E-04	7.572E+11	27	2.47E-04	2.79E+11
35	4.43E-05	2.204E+11	28	1.33E-05	1.50E+10
37	1.08E-04	5.365E+11	30	2.67E-05	3.01E+10
38	4.44E-05	2.208E+11	31	8.22E-05	9.27E+10
43	8.21E-05	4.087E+11	32	1.08E-04	1.21E+11
51	1.26E-04	6.295E+11	33	1.33E-05	1.51E+10
57	4.43E-05	2.206E+11	36	8.20E-05	9.25E+10
60	1.33E-05	6.642E+10	37	4.44E-05	5.01E+10
70	8.21E-05	4.087E+11	38	1.02E-04	1.15E+11
74	8.21E-05	4.089E+11	40	1.33E-05	1.50E+10
84	4.43E-05	2.207E+11	41	9.54E-05	1.08E+11
86	1.33E-05	6.620E+10	45	4.43E-05	5.00E+10
87	1.33E-05	6.635E+10	46	4.43E-05	5.00E+10
91	1.33E-05	6.632E+10	50	8.21E-05	9.26E+10
104	1.33E-05	6.635E+10	56	4.43E-05	5.00E+10
105	1.33E-05	6.632E+10	57	1.33E-05	1.50E+10
114	1.33E-05	6.635E+10	61	2.66E-05	3.00E+10
153	1.33E-05	6.630E+10	63	2.66E-05	3.00E+10
			65	2.67E-05	3.01E+10
			70	1.33E-05	1.50E+10

Now it is necessary to determine the cluster production rate with respect to a specific neutron flux. This requires the PKA production rate be specified. From SPECTER calculations, the displacement cross section of the neutron irradiation was also obtained, which enabled the computation of the total displacement rate (R_d) in tungsten, as defined in Eq. (3),

$$R_d\left[\frac{1}{cm^3 \cdot s}\right] = f\left[\frac{1}{cm^2 \cdot s}\right] s_d\left[cm^2\right] N\left[\frac{1}{cm^3}\right], \tag{3}$$

where $\phi=3.5\times10^{15}$ [$\frac{\text{neutron}}{\text{cm}^2}$/s] , σ_d=51.229 barn , and N=6.3×10^{22} atoms/cm^3 . The displacement cross section for tungsten under neutron irradiation in HFIR has a low value due to the incorporation of thermal neutrons in the neutron flux energy spectrum, which in general do not cause direct displacements through elastic scattering.

Fortunately, there is another way to calculate the displacement rate, as defined in Eq. (4),

$$R_d\left[\frac{1}{cm^3 \cdot s}\right] = I\left[\frac{PKA}{cm^3 \cdot s}\right] P_d\left[\frac{displacements}{PKA}\right], \tag{4}$$

where the displacements per PKA can be computed based on the MD database (P_d=2.27 disp./PKA).

Combining Eqs. (3) and (4) yielded the PKA production rate, 1.12×10^{15} PKA/cm^3/s. Thus, the intra-cascade cluster production probabilities can be obtained by multiplying the values in the second and fifth columns of Table 1 with PKA production rate in the tungsten subject to neutron irradiation at HFIR.

In the present model, all interstitial loops and only single vacancy are considered mobile. Diffusion coefficients of mobile species are required to describe the binary interactions of the binding process of two species (at least one is mobile). Table 2 listed the set of mobility data chosen on empirical basis by considering various studies.

Table 2. Mobility set for interstitial clusters and single vacancy for the modeling of neutron irradiated W

Clusters	V	I_1-I_{10}	I_{11}-I_{20}	I_{21}-I_{30}	I_{31}-I_{40}	I_{41}-I_{50}	$I_{>=51}$
Migration E (eV)	1.30	0.23	0.53	0.63	0.73	0.83	1.35
D_0 (nm^2/s)	1.77×10^{12}			$8.77\times10^{10}/n^{0.5}$			

For the dissociation process of big defect clusters, the emission of single vacancy and SIA is more energetically preferable. The binding energies of single V and SIA to the V and interstitial clusters [8] are shown in Figure 2.

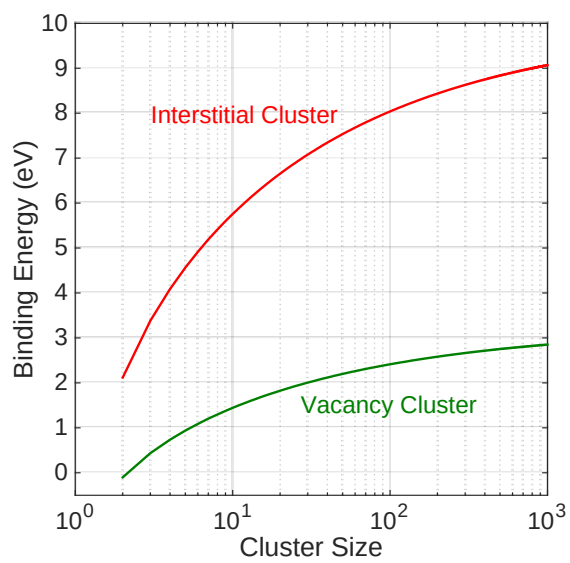

Figure 2. Binding energies of single V and SIA to V and interstitial clusters

Results

ORNL is conducting intense research activities to characterize the microstructure of tungsten neutron-irradiated at HFIR and the resulting mechanical property degradation. 1W25, experiencing low dose (0.03 dpa) and low temperature (90°C) neutron irradiation, was chosen to validate the developed model. Following the cluster dynamics model described above, the vacancy and interstitial cluster population could be predicted, as shown in Figure 3. It can be seen that interstitials undergo significant clustering

even at low doses and low temperature, while vacancies do not, which reflects that the interstitials are much more mobile than vacancies, as shown in Table 2.

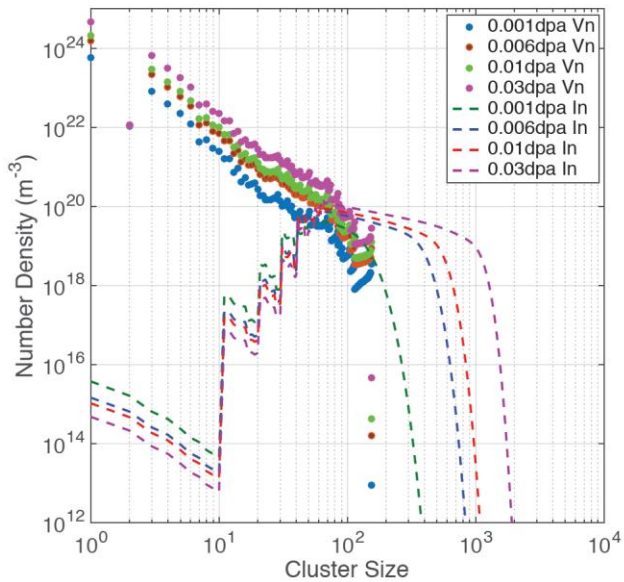

Figure 3. Model predicted volumetric density of interstitial and vacancy clusters plotted as a function of cluster size (n, # of point defects in the cluster) at 90°C.

The validation of model predicted interstitial dislocation loop was realized by comparing with TEM observations. Average dislocation density and size were obtained from TEM. Then a straightforward calculations based on Figure 3 was performed to acquire the information to be compared with TEM. The comparison of experimental data and modeling predictions was shown in Figure 4. It is apparent that the modeling results had a good agreement with the TEM observation for the as-irradiated 1W25 in terms of the interstitial dislocation loops.

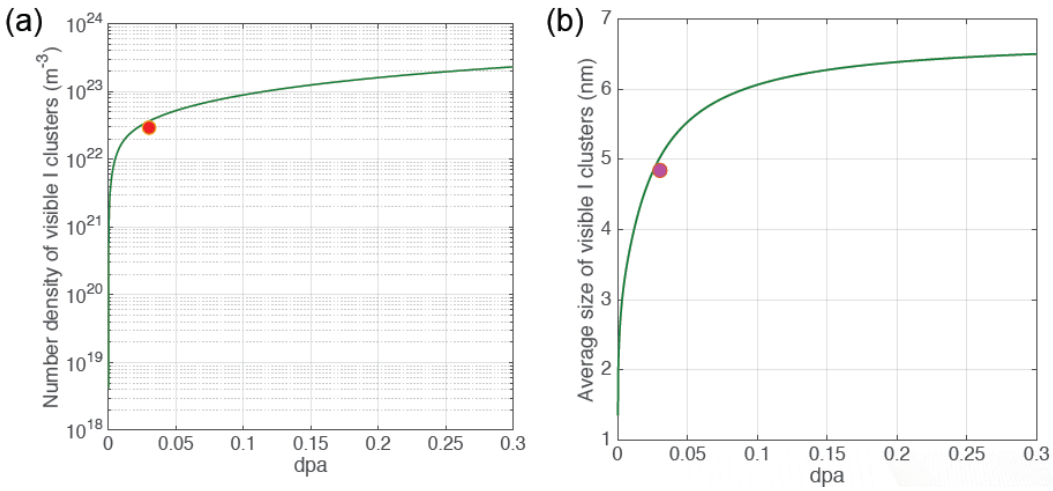

Figure 4. Model prediction of (a) interstitial dislocation loop density and (b) average size of the visible dislocation loop with a TEM resolution of 1.5 nm, as compared to the TEM observations.

In addition to the interstitial dislocation loop, the model predicted vacancy cluster population could be validated by the PAS results. Learning from a recent PAS work on neutron irradiated tungsten, the total vacancy concentration of 1W25 is in the order of 10^{24} m^{-3}, which is consistent with the modeling result,

6.2×10^{24} m^{-3}. Moreover, the PAS also provides the vacancy distribution in a rough way. A straightforward comparison is shown in Figure 5.

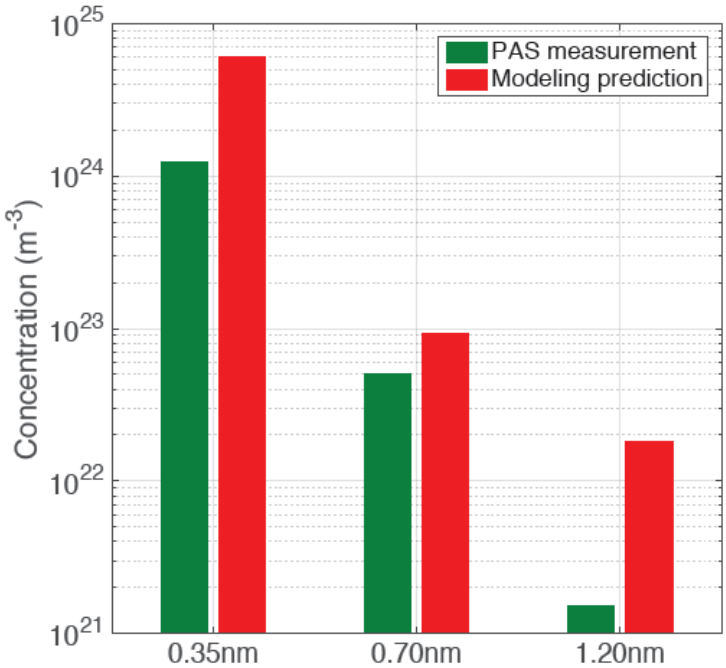

Figure 5. Comparison of modeling prediction and experimental measurements of size distribution of vacancy clusters in as-irradiated 1W25.

There was only one experimental data for both interstitial dislocation loop and vacancy cluster to validate the developed model, which is definitely not sufficient. A recent annealing study of neutron irradiated single crystalline tungsten enabled a more systematic comparison between the PAS results and the modeling results. Following one hour anneals at 400, 500, 650, 800, 1000, 1150, and 1300°C for 1W25, *ex situ* characterization of vacancy defects used positron lifetime spectroscopy, which gave a rough estimation of the vacancy defect population at different annealing stages. The cluster dynamics model was then applied to simulate the corresponding annealing stages. The currently available modeling results are shown in Figure 6.

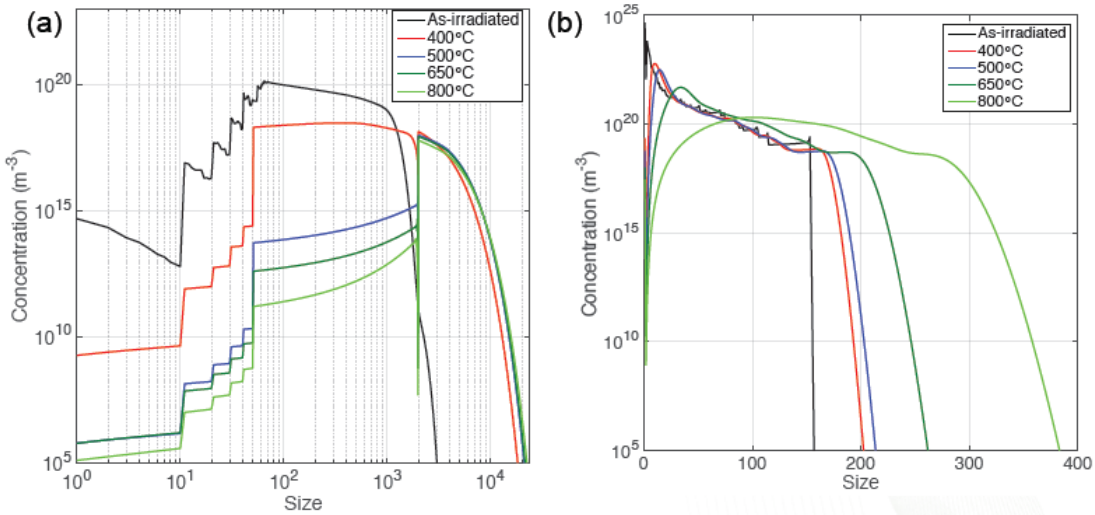

Figure 6. Modeling results of (a) interstitial dislocation loop and (b) vacancy defect cluster at different annealing stages together with the as-irradiated condition.

It is shown in Figure 6(a) that the mobile interstitial dislocation loops decreased with the increasing annealing temperature. After annealed at 400°C for one hour, the loops expanded to larger regime due to the strong combination of the mobile clusters. However, the 500, 650, and 800°C anneals didn't push this process further due to continuously decreasing concentrations of the mobile clusters. With respect to the vacancy cluster, anneals at 400 and 500°C didn't change the distribution dramatically. Starting from 650°C, the vacancy defect cluster moved to larger space and the case of 800°C was more significant.

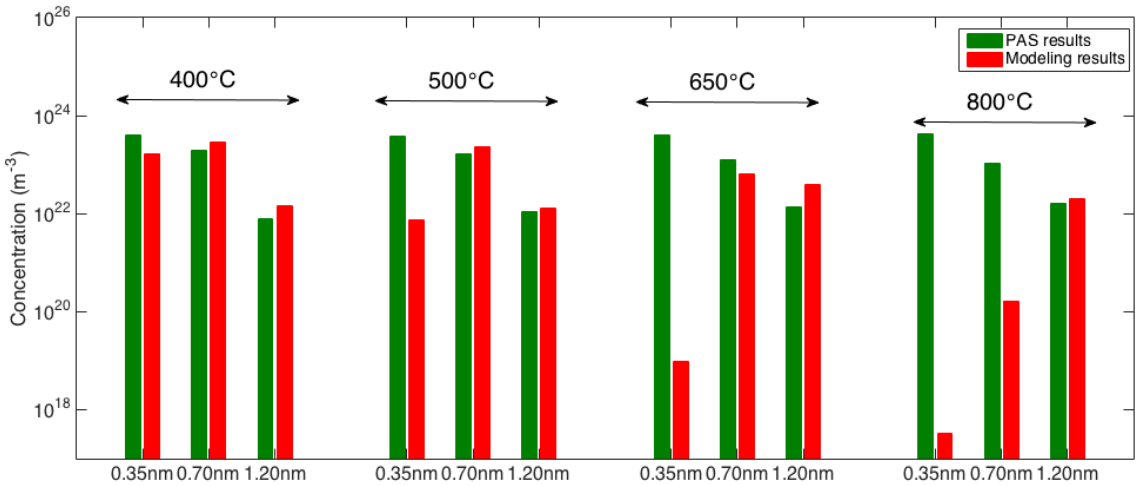

Figure 7. Comparison of the vacancy cluster population obtained from modeling (Red bars) and PAS measurements (Green bars) at different annealing stages.

The vacancy defect population obtained by employing positron annihilation lifetime spectroscopy enabled the validation of the modeling predictions as shown in Figure 7. The modeling predictions of the intermediate and larger voids had a good agreement with the experimentally obtained results. However, the model didn't successfully reproduce the small vacancy cluster evolution when the annealing temperature was higher than 500°C. The small vacancy cluster population obtained from PAS measurement didn't not change obviously, due to the presence of impurity-stabilized vacancy clusters, which was not explicitly included in the model. More work is needed to address the discrepancy between modeling and experimental data.

Planned Work

Up to date, the annealing stages at 400, 500, 650, and 800°C have been simulated by applying the developed cluster dynamics model. The modeling of the remaining three annealing stages, 1000, 1150, and 1300°C, are being performed. Meanwhile, the validation of the vacancy defect cluster was performed by comparing with the PAS measurements for the completed modeling work. In addition, the information of interstitial dislocation loops from TEM observations is necessary to validate the model predictions.

References

[1] Wirth, B.D., et al., Fusion materials modeling: Challenges and opportunities. MRS Bulletin, 2011. 36(03): p. 216-222.

[2] Wirth, B.D., et al., Multiscale modeling of radiation damage in Fe-based alloys in the fusion environment. Journal of Nuclear Materials, 2004. 329-333: p. 103-111.

[3] Wirth, B.D., et al., Modeling defect cluster evolution in irradiated structural materials: Focus on comparing to high-resolution experimental characterization studies. Journal of Materials Research, 2015: p. 1-16.

[4] Hu, X., et al., Modeling of irradiation hardening of iron after low-dose and low-temperature neutron irradiation. Modelling and Simulation in Materials Science and Engineering, 2014. 22(6): p. 065002.

[5] Nandipati, G., et al., Displacement cascades and defect annealing in tungsten, Part III: The sensitivity of cascade annealing in tungsten to the values of kinetic parameters. Journal of Nuclear Materials, 2015.

[6] Ogorodnikova, O.V. and V. Gann, Simulation of neutron-induced damage in tungsten by irradiation with energetic self-ions. Journal of Nuclear Materials, 2015. 460: p. 60-71.

[7] Setyawan, W., et al., Displacement cascades and defects annealing in tungsten, Part I: Defect database from molecular dynamics simulations. Journal of Nuclear Materials, 2014.

[8] Becquart, C.S., et al., Microstructural evolution of irradiated tungsten: Ab initio parameterisation of an OKMC model. Journal of Nuclear Materials, 2010. 403(1-3): p. 75-88.